

Article

# Deactivation of Cu/SSZ-13 NH<sub>3</sub>-SCR Catalyst by Exposure to CO, H<sub>2</sub>, and C<sub>3</sub>H<sub>6</sub>

Xavier Auvray<sup>1</sup>, Oana Mihai<sup>2</sup>, Björn Lundberg<sup>2</sup> and Louise Olsson<sup>1,\*</sup> 

<sup>1</sup> Competence Centre for Catalysis (KCK), Chemical Engineering, Chalmers University of Technology, SE-412 96 Göteborg, Sweden; auvray@chalmers.se

<sup>2</sup> Volvo Car Corporation, SE-405 31 Göteborg, Sweden; oana.mihai@volvocars.com (O.M.); bjorn.lundberg@volvocars.com (B.L.)

\* Correspondence: louise.olsson@chalmers.se

Received: 17 September 2019; Accepted: 1 November 2019; Published: 6 November 2019



**Abstract:** Lean nitric oxide (NO<sub>x</sub>)-trap (LNT) and selective catalytic reduction (SCR) are efficient systems for the abatement of NO<sub>x</sub>. The combination of LNT and SCR catalysts improves overall NO<sub>x</sub> removal, but there is a risk that the SCR catalyst will be exposed to high temperatures and rich exhaust during the LNTs sulfur regeneration. Therefore, the effect of exposure to various rich conditions and temperatures on the subsequent SCR activity of a Cu-exchanged chabazite catalyst was studied. CO, H<sub>2</sub>, C<sub>3</sub>H<sub>6</sub>, and the combination of CO + H<sub>2</sub> were used to simulate rich conditions. Aging was performed at 800 °C, 700 °C, and, in the case of CO, 600 °C, in a plug-flow reactor. Investigation of the nature of Cu sites was performed with NH<sub>3</sub>-temperature-programmed desorption (TPD) and diffuse reflectance infrared Fourier transform spectroscopy (DRIFT) of probe molecules (NH<sub>3</sub> and NO). The combination of CO and H<sub>2</sub> was especially detrimental to SCR activity and to NH<sub>3</sub> oxidation. Rich aging with low reductant concentrations resulted in a significantly larger deactivation compared to lean conditions. Aging in CO at 800 °C caused SCR deactivation but promoted high-temperature NH<sub>3</sub> oxidation. Rich conditions greatly enhanced the loss of Brønsted and Lewis acid sites at 800 °C, indicating dealumination and Cu migration. However, at 700 °C, mainly Brønsted sites disappeared during aging. DRIFT spectroscopy analysis revealed that CO aging modified the Cu<sup>2+</sup>/CuOH<sup>+</sup> ratio in favor of the monovalent CuOH<sup>+</sup> species, as opposed to lean aging. To summarize, we propose that the reason for the increased deactivation observed for mild rich conditions is the transformation of the Cu species from Z<sub>2</sub>Cu to ZCuOH, possibly in combination with the formation of Cu clusters.

**Keywords:** Cu/SSZ-13; NH<sub>3</sub> SCR; aging; deactivation; rich conditions

## 1. Introduction

The need to reduce fuel consumption and greenhouse gas emissions has led to the development of diesel and lean-burn gasoline-powered vehicles. However, this type of engine, operating in excess of air, produces nitric oxides (NO<sub>x</sub>) that cannot be reduced with conventional three-way catalysts. Net oxidizing exhausts require the need for additional reductants to convert NO<sub>x</sub> into nitrogen over a catalyst. In the selective catalytic reduction technology (SCR), the reductant can be hydrocarbons from the fuel (HC-SCR) or ammonia obtained from the hydrolysis of urea (NH<sub>3</sub>-SCR). Cu-exchanged small-pore zeolite is the state-of-the-art catalyst for NH<sub>3</sub>-SCR. In particular, Cu-exchanged zeolite with a chabazite structure has shown improved SCR activity and hydrothermal stability compared to other Cu-exchanged zeolites [1,2]. The combination of NH<sub>3</sub>-SCR with a lean NO<sub>x</sub>-trap catalyst (LNT) has shown enhanced NO<sub>x</sub> reduction and higher N<sub>2</sub> selectivity [3–5]. This system is a promising solution to comply with increasingly stringent emission regulations and to tackle low-temperature

NO<sub>x</sub> emission. In this configuration, however, the SCR catalyst can be subjected to rich conditions and high temperatures during the desulfation of the LNT catalyst. Therefore, aging SCR Cu/zeolite in rich conditions or in lean/rich cycling conditions has attracted attention [6–8]. In our earlier study, we found that aging in the presence of a high-hydrogen concentration proved to be extremely negative for a Cu/SSZ-13 catalyst compared to hydrothermal aging in lean conditions [6]. The rapid and irreversible migration of Cu ions that forms large Cu<sup>0</sup> particles was identified as the cause of the low SCR activity. Moreover, Kim et al. noted an increase in NH<sub>3</sub> oxidation to NO after lean/rich aging at 620 °C [8], which decreases net NO reduction.

The NH<sub>3</sub> SCR reaction process follows a redox cycle of copper cations [9,10]. The oxidation state and location of Cu cations is, therefore, a determining parameter for catalytic activity. In chabazite zeolites, Cu can be found as isolated Cu<sup>2+</sup>, balancing two negative charges of nearby Al atoms in the zeolite framework (Z2Cu), or as [CuOH]<sup>+</sup>, which is connected to one Al (ZCuOH) [11,12]. The Si/Al ratio of the zeolite and the Cu-exchange level influences the partition of these two copper species [13]. Statistically, Si/Al must be low to increase the probability of 2 Al atoms at T-sites in the vicinity of a single Cu cation. Cu<sup>+</sup> that balances one negative charge can be obtained with the autoreduction of Cu<sup>2+</sup>, facilitated with a vacuum or dehydration in an inert atmosphere [12,14–16]. Low Cu loading also increases the fraction of Cu<sup>+</sup> [10]. Cu can be located in various sites of the SSZ-13 framework such as in the CHA cage, in the double 6-member ring cage (d6r), or in the 8-member ring (8MR). As evidenced by DFT calculations, these sites are not equivalent and have different reactivity and interaction with molecules [17–19]. In the d6r, Cu is found as Z2Cu; in 8MR, Cu is found as ZCuOH. Moreover, during SCR reaction conditions these copper species are very mobile [12], which will be discussed more in the following paragraph. The effect of hydrothermal aging in lean and wet conditions has been extensively studied [20–26] since durability of automotive catalysts is a crucial parameter to meet emission standards throughout the lifetime of a vehicle. Under lean hydrothermal conditions, it was found that the state of Cu is altered, which yielded a lower SCR conversion. Upon aging, ZCuOH is converted into Z2Cu, which is more stable [11,13,24]. Cu migration and the formation of Cu oxide clusters have also been reported [20,25].

However, little has been published on the effect of rich conditions on the interconversion of Cu species. Reductant rich exhausts and high temperature can occur in vehicles equipped with a tandem LNT-SCR system during, for instance, desulfation of the LNT. Ligand molecules such as H<sub>2</sub>O and NH<sub>3</sub> have shown the ability to solvate Cu<sup>2+</sup> tethered to a framework Al [10]. The solvated Cu cations become mobile in the CHA cages [27]. In the presence of CO, which is a Lewis base, similar solvation and mobility of Cu<sup>2+</sup> might be possible. High Cu mobility can lead to strong deactivation as we have shown in the presence of 1% H<sub>2</sub> [6]. Since CO is produced during the purge of the LNT catalyst and can be converted into H<sub>2</sub> according to the water-gas shift reaction, it is important to evaluate the consequence of CO and H<sub>2</sub> exposure on Cu/SSZ-13 SCR catalyst.

However, there are to our knowledge, no studies available where the effect of different reductants during rich aging of Cu/SSZ-13 have been examined, which is the objective of the current work. As such, this study investigates the effect of the reductant and temperature on the subsequent SCR and NH<sub>3</sub> oxidation activity of a Cu/SSZ-13 catalyst. DRIFT spectroscopy and NH<sub>3</sub>-temperature-programmed desorption (TPD) provided new insight into the evolution and the nature of the copper species.

## 2. Results and Discussion

### 2.1. SCR Activity of Degreened and Rich-Aged Catalysts

The activity of a Cu/SSZ-13 catalyst for standard SCR is reported in Figure 1 as the conversion of NO. The activity of degreened samples was reproducible, thus indicating reproducible monolith preparation (Figure S1). Therefore, only one curve corresponding to Sample 3 is presented as a reference. The degreened catalyst had low activity below 150 °C and showed a sharp increase in activity between 150 and 200 °C. From 250 to 350 °C, nearly 100% NO conversion was reached before

activity declined at higher temperatures. The effect of various reductants was evaluated at 800 °C and 700 °C. After 8 h of aging at 800 °C, the light-off temperature increased significantly and the maximum NO conversion attained was lower. At 800 °C, the nature of the gas atmosphere played an important role, which is depicted in Figure 1. It is clear that reducing atmosphere causes more severe aging than lean atmosphere. In addition, the reducing agent also plays an important role. Activity deterioration was more pronounced with 2000 ppm H<sub>2</sub> (and 10% H<sub>2</sub>O, 10% CO<sub>2</sub>, 500 ppm NO) than with 2000 ppm CO (and 10% H<sub>2</sub>O, 10% CO<sub>2</sub>, 500 ppm NO), especially in the temperature window of 300–400 °C. Earlier, we have demonstrated that a high concentration of H<sub>2</sub> (1%) causes tremendous deactivation of Cu/SSZ-13 due to migration and agglomeration of exchanged Cu that forms large particles outside the zeolite framework [6]. Interestingly, also lower concentrations of H<sub>2</sub> (2000 ppm) were found in this study to cause severe deactivation. The combination of CO and H<sub>2</sub> led to the lowest activity below 350 °C and this combination seemed to affect the low-temperature mechanism more than H<sub>2</sub> or CO alone. At higher temperatures, however, the samples aged with CO + H<sub>2</sub> and H<sub>2</sub> presented similar activity. The nature of the reductant was found to play a major role in the deactivation process of Cu/SSZ-13 at 800 °C and the results clearly show that the deactivation is significantly higher in rich compared to lean conditions that use low reductant concentrations.

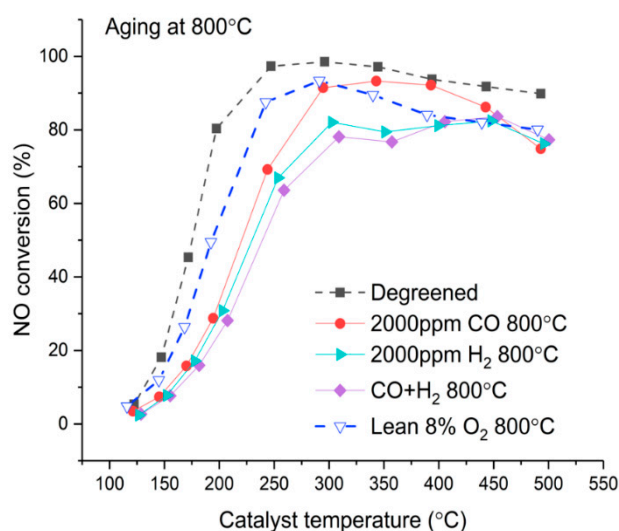


**Figure 1.** Effect of reductant nature on standard selective catalytic reduction (SCR) activity for catalysts aged 8 h at 800 °C. NO conversion measured in the range of 125–500 °C on degreened catalyst. Experimental conditions: 500 ppm NH<sub>3</sub>, 500 ppm NO, 8% O<sub>2</sub>, 5% H<sub>2</sub>O in Ar, total flow 3.5 L/min.

The results obtained after aging at 700 °C are shown in Figure 2. The consequence of aging on activity was moderate and characterized by a moderate shift of the light-off towards higher temperatures. However, less deactivation was noted above 250 °C. The results in Figure 2 indicate that CO, H<sub>2</sub>, CO + H<sub>2</sub>, and C<sub>3</sub>H<sub>6</sub> have equal effects on deactivation at 700 °C. It should be noted that the catalyst aged with H<sub>2</sub> showed lower activity, from 300 °C, than the other samples after degreening. The apparent decrease observed in Figure 2 for the sample above 300 °C is, consequently, not related to aging, but to small variations in the fresh monolith. Despite the slight influence of the reducing agent, the conditions played a role in aging at 700 °C. Figure S2 represents the SCR activity of a catalyst aged in lean conditions at 700 °C and shows less-pronounced deactivation at low temperature for this sample than for the rich-aged samples. Note that this monolith was prepared from another Cu/SSZ-13 batch.

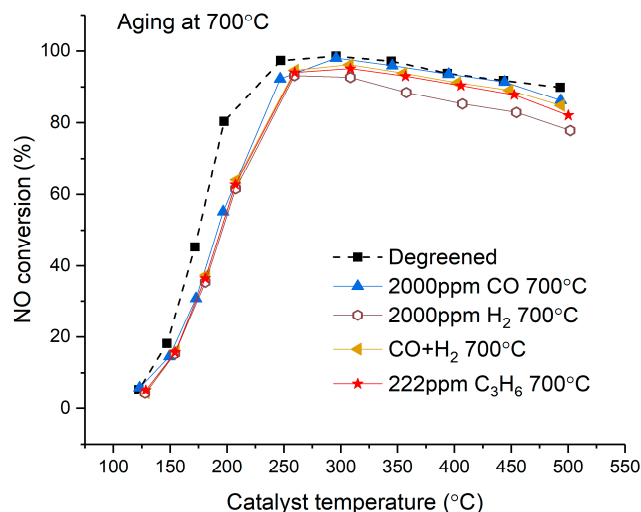


**Figure 2.** Effect of reductant nature on standard SCR activity for catalysts aged 8 h at 700 °C. NO conversion measured in the range of 125–500 °C on degreened catalyst. Experimental conditions: 500 ppm NH<sub>3</sub>, 500 ppm NO, 8% O<sub>2</sub>, 5% H<sub>2</sub>O in Ar, total flow 3.5 L/min.

The effect of aging temperature is shown in more detail in Figure 3 in which the SCR activity of fresh catalyst is compared with catalysts aged in 2000 ppm CO (and 10% H<sub>2</sub>O, 10% CO<sub>2</sub>, 500 ppm NO) at 600, 700, and 800 °C. The results show that the deactivation is strongly linked to aging temperature with a greater deactivation measured after aging at a higher temperature, as expected. However, it is remarkable that aging at only 600 °C with 2000 ppm CO (and 10% H<sub>2</sub>O, 10% CO<sub>2</sub>, 500 ppm NO) leads to a loss in activity, which illustrates the specific impairing effect of CO and reducing conditions. After aging at 700 °C, deactivation was only significant below 300 °C. Aging at 800 °C was required to influence high-temperature SCR activity.

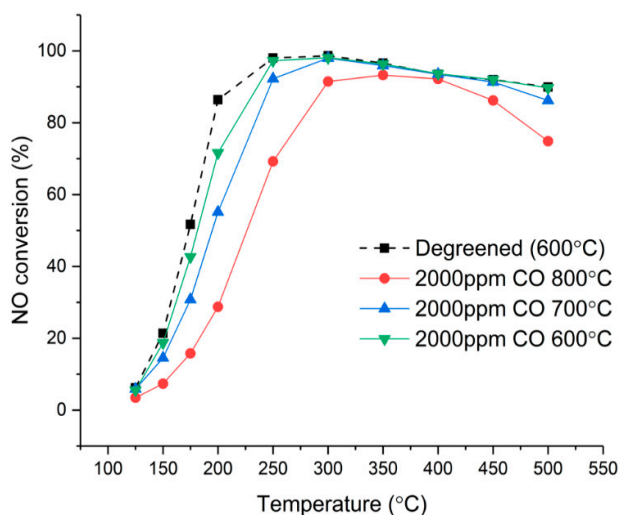


**Figure 3.** Effect of aging temperature on standard SCR activity for catalysts aged with 2000 ppm CO for 8 h. NO conversion measured in the range of 125–500 °C on degreened catalysts and catalysts aged at 600 °C, 700 °C, and 800 °C. Experimental conditions: 500 ppm NH<sub>3</sub>, 500 ppm NO, 8% O<sub>2</sub>, 5% H<sub>2</sub>O in Ar, total flow 3.5 L/min.

## 2.2. NH<sub>3</sub>-TPD Analysis

NH<sub>3</sub> TPD was carried out to characterize the amount and strength of acid sites. In Cu-exchanged zeolites, Lewis acid sites are mainly isolated Cu<sup>2+</sup> and Brønsted acid sites are the Al-OH-Si bridges. The degreened samples showed similar TPD profiles. Therefore, only two profiles are used for reference

in Figure 4a,b. The degreened catalysts showed two NH<sub>3</sub> desorption peaks at ca. 300 and 390 °C. These were assigned to Lewis acid sites and Brønsted acid sites, respectively [28]. In addition, NH<sub>3</sub> strongly adsorbed on Cu<sup>2+</sup> have also contributed to the high-temperature desorption peak [28,29]. Aging at 800 °C significantly decreased the NH<sub>3</sub> storage capacity (Figure 4a) of both desorption peaks, but the high-temperature peak decreased to greater extent. The combination of H<sub>2</sub> and CO led to the lowest NH<sub>3</sub> storage. The multiple possible locations for Cu<sup>2+</sup> in the zeolite framework make the NH<sub>3</sub> desorption feature complex. Figure 4a shows a NH<sub>3</sub> desorption peak at 305 °C for the catalyst aged with CO. The desorption temperature for the catalysts aged with H<sub>2</sub> and H<sub>2</sub> + CO was significantly higher at 325 °C, indicating the influence of the aging atmosphere on the population of the Cu species. TEM analysis coupled with EDS mapping was performed on the catalyst aged with CO at 800 °C to check for possible growth of Cu particles. Brighter areas of 2–3 nm in diameter with a composition slightly richer in Cu than the surrounding matrix were detected. However, they were too small to conduct a full EDS mapping of the catalyst particles and conclude accurately on the presence and quantity of Cu particles. In our earlier study, more severe aging was performed using 1% H<sub>2</sub> (and 10% H<sub>2</sub>O, 10% CO<sub>2</sub>, 500 ppm NO) [6]. Due to the high H<sub>2</sub> concentration the Cu migration was further promoted, and clear large Cu particles were observed using STEM-EDS. Thus, it is likely that the observed bright areas for the STEM analysis for aging in milder conditions are due to copper clusters, although it cannot be confirmed by EDS, due to the resolution of our EDS measurements.

Figure 4b represents the NH<sub>3</sub> TPD after various aging conditions at 700 °C and aging with CO at 600 °C. Despite moderate activity loss after aging at 700 °C (Figure 2), all catalysts lost a great amount of high-temperature NH<sub>3</sub> storage sites, which mostly corresponded to Brønsted acid sites. It is interesting that the catalyst aged with 2000 ppm CO at 600 °C, which showed minor SCR deactivation, lost a large amount of storage sites in the high-temperature region. This result demonstrates the non-trivial relationship between SCR activity and NH<sub>3</sub> storage sites, especially the sites that strongly bond NH<sub>3</sub>. After aging at 700 °C, all samples suffered similar deactivation of low-temperature SCR and similar loss of mostly Brønsted acid sites. The loss of Brønsted acid sites indicates dealumination of the zeolite [25], however, dealuminated CHA zeolites can preserve their crystalline structure [6,22].

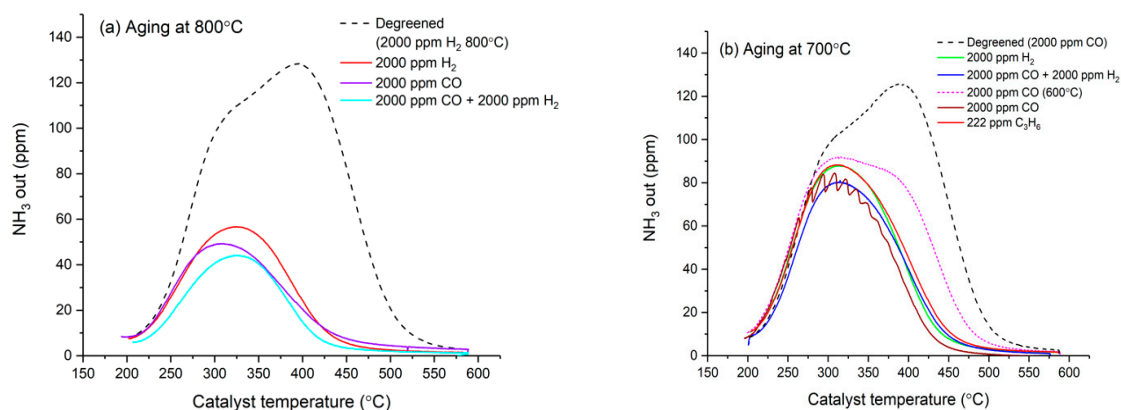


**Figure 4.** NH<sub>3</sub>-temperature-programmed desorption (TPD). (a) Catalysts aged at 800 °C and (b) catalysts aged at 700 °C and 600 °C. NH<sub>3</sub> adsorption conditions: 500 ppm NH<sub>3</sub>, 5% H<sub>2</sub>O in Ar, total flow 3.5 L/min, 30 min at 200 °C. Desorption conditions: 5 °C/min up to 600 °C, 3.5 L/min Ar.

### 2.3. NH<sub>3</sub> Oxidation Activity

Figure 5 shows the NH<sub>3</sub> conversion CO measured during the NH<sub>3</sub> oxidation test performed on monolithic catalysts. The production of N<sub>2</sub>O and NO never exceeded 5 ppm, indicating high selectivity to N<sub>2</sub>. Representative activity profiles of the degreened catalysts are shown with dashed lines in Figure 5a,b. The activity remained below 25% up to 400 °C and seemed to level off. Above 400 °C, however, activity increased sharply with temperature to reach nearly 100% at 500 °C. This dual behavior suggests two different mechanisms for ammonia oxidation on degreened catalyst. After aging at 800

°C, the activity increased progressively with temperature throughout the whole temperature range and the low-temperature feature of the degreened catalyst disappeared. Aging with CO promoted  $\text{NH}_3$  oxidation to  $\text{N}_2$  from 400 °C, unlike the SCR. This effect is specific to CO aging at 800 °C since  $\text{H}_2$  and  $\text{H}_2 + \text{CO}$  lead to the deactivation of both SCR and  $\text{NH}_3$  oxidation throughout the whole temperature range. The activity measured after aging at 700 °C is shown in Figure 5b. It can be seen in that figure that the promoting effect of CO aging was absent following aging at 700 °C and 600 °C. Aged catalysts displayed similar profiles as degreened ones up to 400 °C, i.e., when the low-temperature mechanism applies. However, at higher temperatures, aging at 700 °C decreased the ammonia oxidation for all reductants. Aging in CO at 600 °C consistently caused less modification of the catalyst activity than at aging at 700 °C and 800 °C.

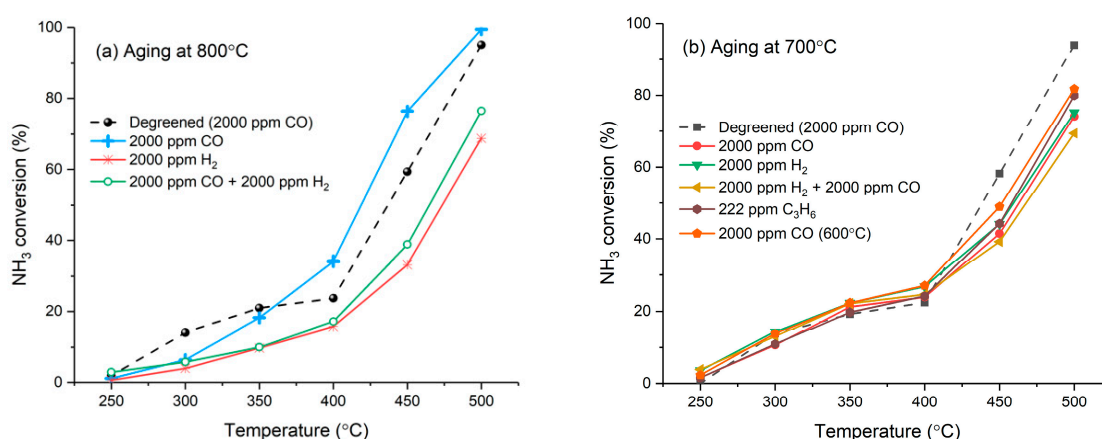


**Figure 5.**  $\text{NH}_3$  oxidation in the range of 250–500 °C. (a) Catalysts aged at 800 °C and (b) catalysts aged at 700 °C and 600 °C. Experimental conditions: 500 ppm  $\text{NH}_3$ , 8%  $\text{O}_2$ , 5%  $\text{H}_2\text{O}$  in Ar, total flow 3.5 L/min.

#### 2.4. DRIFT Spectroscopy Study of $\text{NH}_3$ Adsorption

$\text{NH}_3$  adsorption, monitored with DRIFT spectroscopy, provided additional information regarding the state of copper sites, the nature of acid sites, and the extent of dealumination.  $\text{NH}_3$  adsorption was performed at 150 °C for 20 min on dehydrated catalysts. Figure 6 presents the spectra obtained at the end of exposure of degreened and aged catalysts to  $\text{NH}_3$  in the spectral region corresponding to T-O-T vibrations. Since the degreened powder was pure and the aged catalysts contained  $\approx 75$  wt % cordierite, the reported signal intensity of degreened catalyst was divided by a factor of four in order to facilitate comparison. The presence of exchanged Cu is known to disturb the vibration of a zeolite framework. When  $\text{NH}_3$  interacts with exchanged Cu, the Cu-induced perturbation of the T-O-T vibration weakens, and negative IR absorption bands appear [11]. Two Cu species were identified:  $\text{Cu}^{2+}$  bound to two  $\text{Al}^-$ , denoted Z2Cu; and  $[\text{Cu}(\text{OH})]^+$  bound to one  $\text{Al}^-$ , denoted ZCuOH. The degreened Cu/SSZ-13 spectra showed two negative bands centered at 900  $\text{cm}^{-1}$  and 950  $\text{cm}^{-1}$ , respectively, the former being more pronounced. The band at 900  $\text{cm}^{-1}$  was assigned to the Z2Cu sites, connected to two Al, while the band at 950  $\text{cm}^{-1}$  was assigned to ZCuOH [11,30].

The results after aging at 800 °C are presented in Figure 6a, where a clear effect on the intensity of these bands upon aging is visible. The lowest intensity was obtained after aging in 2000 ppm  $\text{H}_2$ , suggesting the loss of exchanged Cu in these aging conditions. This result is in line with the lower conversion noted after  $\text{H}_2$  aging than after CO aging. The intensity ratio of the two bands was modified after aging at 800 °C. The ZCuOH band at 950  $\text{cm}^{-1}$  was poorly resolved and, in the case of CO aging, it resembled a shoulder of the 900  $\text{cm}^{-1}$  band. Luo et al. [11] and Song et al. [30] have observed the conversion of ZCuOH sites into Z2Cu sites with hydrothermal aging. This phenomenon was reproduced by aging in lean conditions in our study (data not shown). This appears not to occur when aging is conducted in a rich environment, since both FTIR peaks decreased in intensity. Instead,

it is suggested that a fraction of exchanged Cu was reduced and migrated outside the zeolite. This was found for aging with 1% H<sub>2</sub> [6]. Figure 6b shows that, after aging at 700 °C in either H<sub>2</sub> or H<sub>2</sub> + CO, both absorption bands were more intense, and the 950 cm<sup>-1</sup> was well-resolved. Aging in CO at 600 °C yielded the greatest band intensity, demonstrating the milder effect of lower aging temperature on the amount of exchanged Cu sites. Based on the relative intensity of the bands at 900 and 950 cm<sup>-1</sup>, the DRIFTS results indicate an increase in the ZCuOH/Z<sub>2</sub>Cu ratio with aging in rich conditions, which is the opposite of what has been reported for hydrothermal aging [11,30]. To summarize, we propose that the reason for the increased deactivation observed for mild rich conditions is the transformation of the Cu species from Z<sub>2</sub>Cu to ZCuOH.

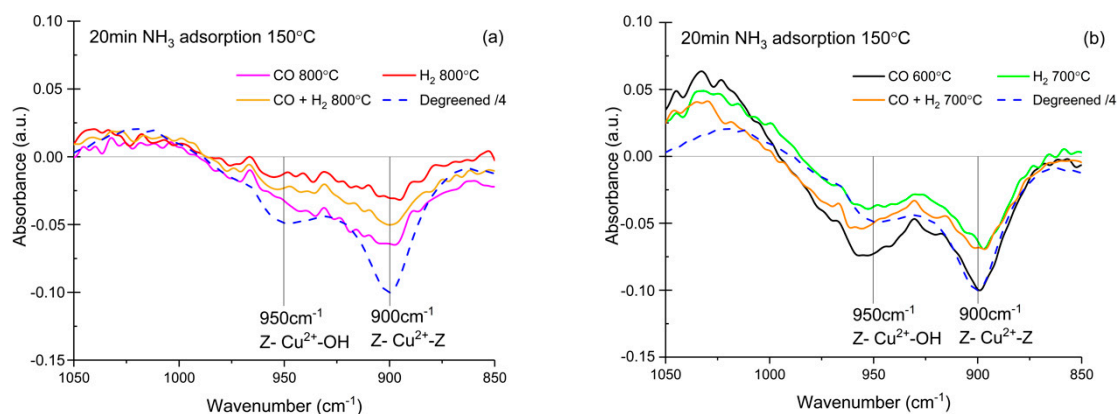


**Figure 6.** Diffuse reflectance infrared Fourier transform spectroscopy (DRIFT) spectra of the T-O-T vibration region (1050–850 cm<sup>-1</sup>) after NH<sub>3</sub> adsorption at 150 °C (1000 ppm, 20 min). (a) Catalysts aged at 800 °C and (b) catalysts aged at 700 °C and 600 °C. The catalysts were pretreated at 500 °C (8% O<sub>2</sub> in Ar, 30 min). The degreened catalyst signal was divided by four and the aged catalysts were crushed monolith, containing ca. 75 wt % cordierite.

Figure 7 shows the N-H stretching vibration region of the DRIFT spectra where two main features can be seen at 1622 cm<sup>-1</sup> and 1462 cm<sup>-1</sup> on the degreened sample. The former was assigned to NH<sub>3</sub> coordinated to Cu<sup>2+</sup> while the latter was assigned to NH<sub>4</sub><sup>+</sup>, indicating the protonation of NH<sub>3</sub> on Brønsted acid sites [11,31–33]. These two bands were used to titrate Lewis and Brønsted sites on Cu-exchanged zeolites. Before aging, the absorbance band caused by NH<sub>4</sub><sup>+</sup> at 1462 cm<sup>-1</sup> was slightly more intense than the Lewis band at 1622 cm<sup>-1</sup>. However, after aging at 800 °C, Figure 7a shows that the Lewis site band at 1622 cm<sup>-1</sup> became more pronounced, indicating the loss of Brønsted acid sites. The intensity ratio 1622 cm<sup>-1</sup>/1462 cm<sup>-1</sup> is dependent on aging conditions, and it was higher after H<sub>2</sub> aging, which yielded very weak Brønsted site band. The Brønsted band also shifted towards lower wavenumbers after aging at 800 °C. At lower aging temperatures (Figure 7b), a similar shift was noted, even after aging in CO at 600 °C. However, for aging with CO at 600 °C, the intensity of the Brønsted band (1462 cm<sup>-1</sup>) was very strong. Moreover, for the NH<sub>3</sub> TPD experiments the CO aging at 600 °C, it resulted in less aging compared to the other samples. However, a clear loss of Brønsted acid sites was still visible, which was not the case for the DRIFT data. This demonstrates that the assignment of the NH<sub>3</sub> desorption peaks is not a trivial task and that a fraction of the high-temperature desorption peak is due to NH<sub>3</sub> strongly adsorbed on Cu. These species were affected by aging in CO at 600 °C.

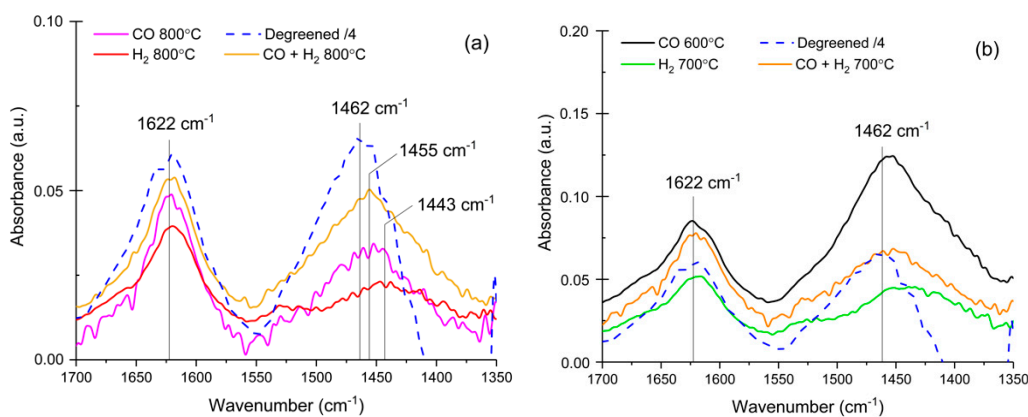


**Figure 7.** DRIFT spectra of  $\text{NH}_3$  adsorption at  $150\text{ }^\circ\text{C}$  (1000 ppm, 20 min) recorded after pretreatment at  $500\text{ }^\circ\text{C}$  (8%  $\text{O}_2$  in Ar, 30 min). **(a)** Catalysts aged at  $800\text{ }^\circ\text{C}$  and **(b)** catalysts aged at  $700\text{ }^\circ\text{C}$  and  $600\text{ }^\circ\text{C}$ . The degreened catalyst signal was divided by 4, and the aged catalysts were crushed monolith, containing ca. 75 wt % cordierite.

### 2.5. NO Adsorption on Oxidized Cu/SSZ-13

To study the nature of Cu sites in further detail, NO adsorption was performed at  $30\text{ }^\circ\text{C}$  in the DRIFT cell after an oxidizing pretreatment at  $500\text{ }^\circ\text{C}$ . NO is a suitable probe molecule that binds to Cu and allows discernment of the redox state and possibly the location of Cu. Figure 8 presents the spectra collected after a 20-min exposure to NO. Nitrates and adsorbed  $\text{NO}_2$  were formed on the surface of the catalyst as attested by the absorption bands in the region  $1500\text{--}1700\text{ cm}^{-1}$  on all catalysts (not shown). A broad and intense feature, composed of three peaks at  $2213$ ,  $2183$ , and  $2158\text{ cm}^{-1}$ , was found on degreened and aged catalysts at  $800\text{ }^\circ\text{C}$ . These peaks were assigned to  $\text{NO}^+$  in cationic sites ( $2158\text{ cm}^{-1}$ ) and  $\text{NO}^+\text{NO}_2$  adducts ( $2213$ ,  $2183\text{ cm}^{-1}$ ) [34,35]. A less intense band, attributed to NO adsorbed on isolated  $\text{Cu}^{2+}$  [20,36,37], was found in the  $1850\text{--}1950\text{ cm}^{-1}$  region. The degreened catalyst showed a peak at  $1913\text{ cm}^{-1}$  and an unresolved shoulder at higher wavenumbers. The sharp peak at  $1948\text{ cm}^{-1}$ , corresponding to NO adsorbed on  $\text{Cu}^{2+}$  in the 6-member ring reported by Szanyi et al. [36,37] and Kim et al. [21], was not present on either the degreened or aged catalysts, but a shoulder in this region was found on the degreened sample. Aging at  $800\text{ }^\circ\text{C}$  in reducing conditions provoked a shift to lower wavenumbers of the  $1913\text{ cm}^{-1}$  peak, with the growth of a new peak at  $1895\text{ cm}^{-1}$ , as well as the growth of a shoulder at  $1866\text{ cm}^{-1}$ . The N-O vibration frequency correlates with the  $\text{Cu}^{2+}$  site on which NO is adsorbed. This signals a shift in  $\nu\text{NO}$  indicates the modification of Cu sites. DFT and FTIR results have suggested that  $\nu\text{NO}$  is higher for NO adsorbed on Z2Cu than NO adsorbed on ZCuOH in Cu/SSZ-13 zeolite [17]. The shift of  $\text{Cu}^{2+}\text{-NO}$  and the rise of a peak at  $1866\text{ cm}^{-1}$  suggest that aging in rich conditions changed the distribution of Cu sites in favor of ZCuOH. In addition, the peak at  $1895\text{ cm}^{-1}$  has been observed by Giordanino et al., who assigned it to a monovalent complex likely to be  $[\text{CuOH}]^+$  [16].

During NO adsorption, bands around  $1900\text{ cm}^{-1}$  and  $2158\text{ cm}^{-1}$  developed immediately and reached a maximum after 10 or 15 min before starting to decline during the last 5 min of NO exposure. The bands diminished severely during the subsequent Ar step, except for the degreened catalyst, which showed weak adsorption or subsequent oxidation of NO into nitrates or  $\text{NO}_2$  adsorbed. Both characteristic bands increased throughout the NO step and the band at  $1629\text{ cm}^{-1}$  ( $\text{NO}_2$  ads) remained constant or increased slightly when the NO feed was cut off. Similar observations were made after aging at  $700\text{ }^\circ\text{C}$  in  $\text{H}_2$  and  $\text{CO} + \text{H}_2$  and at  $600\text{ }^\circ\text{C}$  in CO (Figure 8b). The shift of the  $\text{NO-Cu}^{2+}$  band related to the degreened sample and was also observed, although less pronounced. The broad feature at  $2150\text{--}2250\text{ cm}^{-1}$  was composed of the same three peaks with a more even intensity between  $\text{NO}^+$  ( $2158\text{ cm}^{-1}$ ) and  $\text{NO} + \text{NO}_2$  adducts ( $2213$ ,  $2183\text{ cm}^{-1}$ ). No sign of  $\text{Cu}^+$ , characterized by a band at ca.  $1810\text{ cm}^{-1}$  [21,36–38], was detected, which can be expected after an oxidizing pretreatment [14]. However, this means that the observed  $\text{NO}^+$  was not formed by a reduction of  $\text{Cu}^{2+}$  with NO.

To conclude, the results from the NO DRIFTS is in line with the NH<sub>3</sub> DRIFTS where the Cu species are transformed from Z2Cu to ZCuOH, which is opposite compared to lean aging. This could be the reason for the increased aging observed with mild rich conditions compared to lean conditions (Figure 1).

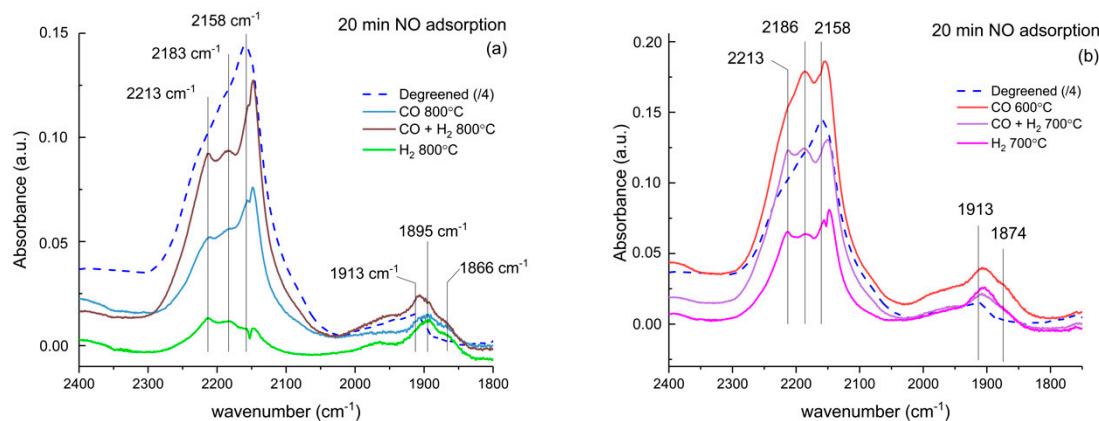


**Figure 8.** DRIFT spectra of NO adsorption at 30 °C (1000 ppm, 20 min) recorded after pretreatment at 500 °C (8% O<sub>2</sub> in Ar, 30 min). (a) Catalysts aged at 800 °C, and (b) catalysts aged at 700 and 600 °C.

### 3. Materials and Methods

#### 3.1. Catalyst Preparation

The zeolite support was synthesized by conversion of Y zeolite, according to the procedure described by Zones et al. [39]. Sodium trisilicate (250 g, Na<sub>2</sub>SiO<sub>3</sub>, VWR) and deionized water (320 g, Millipore) were poured into 200 mL of 1 M NaOH solution, prepared by dissolving NaOH pellets (Sigma Aldrich, >98% anhydrous pellets, St. Louis, MO, USA) in deionized water. After 15 min of stirring, 25 g of zeolite Y (Zeolyst, CBV720) was added to the solution and stirred for 30 min at room temperature. Finally, 105 g of the structure-directing agent (SDA), N,N,N-trimethyl-1-adamantanamine iodide (TMAAI, ZeoGen SDA 2825), was added to the solution. Before being transferred to the Teflon cup of a Parr stainless steel autoclave, the slurry was stirred constantly for 30 min. Hydrothermal aging was carried out in autoclaves filled up to 2/3 of their volume at 140 °C in an oven for six days without mechanical stirring. The solid fraction was then separated with centrifugation and washed repeatedly with deionized water until the solution reached a neutral pH. The powder was then dried for at least 12 h at room temperature and calcined for 8 h at 550 °C at a heating rate of 0.5 °C/min.

The sodium form of the zeolite (Na/SSZ-13) was then ion-exchanged twice with ammonium nitrate. The zeolite powder was slowly poured into a volume of ammonium nitrate solution (2 M) corresponding to 33.33 mL/g of zeolite. The mixture was heated and maintained at 80 °C in an oil bath for 15 h under stirring. The powder was collected with centrifugation and washed with deionized water until the pH was neutral. The powder was dried for 12 h at room temperature and the ion-exchange and washing procedure was carried out a second time before Cu exchange. A copper nitrate solution (0.2 M) was prepared by dissolving copper nitrate hemi(penta-hydrate) (CuN<sub>2</sub>O<sub>6</sub>·2.5H<sub>2</sub>O, Sigma-Aldrich, St. Louis, MO, USA) in deionized water. The volume of solution employed was 100 mL for 3 g of NH<sub>4</sub><sup>+</sup>-exchanged SSZ-13. After washing and subsequent drying for at least 12 h, the Cu-exchanged SSZ-13 powder was calcined for 4 h at 550 °C (5 °C/min heating rate). The final elemental composition was determined with inductively-coupled plasma atomic emission spectroscopy (ICP-AES, performed at ALS Scandinavia, Luleå, Sweden). The copper content was 1.63 wt %, and the Si/Al ratio was 18.

Activity tests and NH<sub>3</sub>-TPD were performed on monolithic catalysts made of cordierite monolithic substrate (400 cpsi, Corning, Corning, NY, USA) coated with a blend of 95 wt % Cu/SSZ-13 and 5 wt % binder (Disperal P2, Sasol, Johannesburg, South Africa). The coating procedure consisted of immersing the monolith in a slurry containing the solid phase (catalyst + binder) dispersed in a liquid solvent

(50 wt % water + 50 wt % ethanol). The liquid-to-solid ratio was  $\approx 4$ , initially. Except during the monolith dipping step, the slurry was stirred. The monolith was continuously rotated and flipped under an air stream ( $\approx 50\text{ }^{\circ}\text{C}$ ) to ensure homogenous drying and deposition of the washcoat. The washcoated monolith was then dried under a hot-air flow ( $\approx 500\text{ }^{\circ}\text{C}$ ) for 1 min to ensure complete evaporation of the solvent before weight measurement. The dipping and drying procedure was repeated until  $\approx 750\text{ mg}$  washcoat was deposited on the monolith. The monolith was 2 cm long and its diameter was 2 cm.

### 3.2. Activity Test (SCR, $\text{NH}_3$ Oxidation, and $\text{NH}_3$ -TPD)

A synthetic gas bench plug-flow reactor was used to carry out three types of experiments on the washcoated monoliths: standard SCR and  $\text{NH}_3$  oxidation activity measurements and  $\text{NH}_3$ -temperature-programmed desorption (TPD). The sample was wrapped in quartz wool to prevent gas bypassing it and placed in a horizontal quartz tube reactor (Technical Glass Product Inc., Painesville Twp., OH, USA). The heating was provided with an electrical resistance coiled around the tube and connected to a power supply. A thick layer of quartz wool surrounding the reactor tube provided thermal insulation. The temperature was measured with two thermocouples inserted at the outlet of the reactor. One thermocouple measured the temperature of the inlet gas, ca. 1 cm upstream of the catalyst and steered the heating system (Eurotherm, Worthing, UK). The second thermocouple was inserted at the center of the monolith to measure the catalyst temperature. Gases were diluted in argon, which was the carrier gas in all experiments. The desired gas flow rates were delivered with mass flow controllers (Bronkhorst, Ruurlo, Netherlands), and water vapor was generated with controlled evaporation and a mixing system (CEM-system, Bronkhorst Ruurlo, Netherlands). The outlet gas composition was analyzed using a calibrated gas FTIR spectrometer equipped with a 200 mL gas cell with a 5.11-m effective pathlength (Multigas 2030, MKS Instruments Inc., Andover, MA, USA). This allowed the quantitative measurement of  $\text{NH}_3$ , NO,  $\text{NO}_2$ ,  $\text{N}_2\text{O}$ ,  $\text{H}_2\text{O}$ , CO,  $\text{C}_3\text{H}_6$ , and  $\text{CO}_2$ .

The catalysts were degreened in the reactor for 3 h at  $600\text{ }^{\circ}\text{C}$  in a gas flow containing 500 ppm NO, 500 ppm  $\text{NH}_3$ , 8%  $\text{O}_2$ , 5%  $\text{H}_2\text{O}$ , balanced by Ar for a total flow of 3.5 L/min. A total flow of 3.5 L/min, corresponding to a gas hourly space velocity (GHSV) of  $33,423\text{ h}^{-1}$ , was used in all experiments conducted on monolithic catalysts. SCR,  $\text{NH}_3$  oxidation, and  $\text{NH}_3$ -TPD measurements were preceded by a 20-min oxidation step at  $500\text{ }^{\circ}\text{C}$  (8%  $\text{O}_2$  and 5%  $\text{H}_2\text{O}$  in Ar). Standard SCR was performed in the range  $125\text{--}500\text{ }^{\circ}\text{C}$  with the same gas composition as the degreening. The conversion reported at each temperature was measured after 40 min to ensure steady-state operation. The ammonia direct-oxidation activity was measured between  $200\text{ }^{\circ}\text{C}$  and  $500\text{ }^{\circ}\text{C}$  with 500 ppm  $\text{NH}_3$  and 8%  $\text{O}_2$  in the presence of 5%  $\text{H}_2\text{O}$ .  $\text{NH}_3$ -TPD consisted of 1 h  $\text{NH}_3$  adsorption at  $200\text{ }^{\circ}\text{C}$  (500 ppm  $\text{NH}_3$  and 5%  $\text{H}_2\text{O}$ ) followed by an argon step of 20 min to flush loose  $\text{NH}_3$ . The temperature of the catalyst was then raised at a controlled pace ( $5\text{ }^{\circ}\text{C}/\text{min}$ ) of 3.5 L/min Ar to desorb  $\text{NH}_3$ .

### 3.3. Aging

The catalysts were aged in the reactor described above for 8 h in a gas flow containing 10%  $\text{H}_2\text{O}$ , 10%  $\text{CO}_2$ , 500 ppm NO, and a reductant species ( $\text{CO}$ ,  $\text{H}_2$ ,  $\text{C}_3\text{H}_6$ ). Each sample was assigned a reductant and aging conditions that are summarized in Table 1. To simulate the exhaust composition during the deSOx period of LNT catalysts, aging in the presence of 2000 ppm CO was studied. Then, following the thermodynamic equilibrium of the water-gas shift reaction ( $\text{CO} + \text{H}_2\text{O} \leftrightarrow \text{H}_2 + \text{CO}_2$ ), aging in a CO/ $\text{H}_2$  equimolar mixture and  $\text{H}_2$  alone was also studied at  $800\text{ }^{\circ}\text{C}$  and  $700\text{ }^{\circ}\text{C}$ . Finally,  $\text{C}_3\text{H}_6$  was studied as a reductant in the proportion required to reduce the same amount of  $\text{O}_2$  as 2000 ppm CO, namely 222 ppm  $\text{C}_3\text{H}_6$ .

**Table 1.** Reaction conditions during aging. Note that in all aging conditions, 10% H<sub>2</sub>O, 10% CO<sub>2</sub>, and 500 ppm NO were always present.

Sample	Reductant	Aging Temperature (°C)
1	2000 ppm CO	600
2	2000 ppm CO	700
3	2000 ppm CO	800
4	2000 ppm H <sub>2</sub>	700
5	2000 ppm H <sub>2</sub>	800
6	2000 ppm H <sub>2</sub> + 2000 ppm CO	700
7	2000 ppm H <sub>2</sub> + 2000 ppm CO	800
8	222 ppm C <sub>3</sub> H <sub>6</sub>	700

### 3.4. DRIFT Measurements

NH<sub>3</sub> and NO adsorption were conducted on powder samples placed in a heated Praying Mantis DRIFT cell (Harrick Scientific Products, Pleasantville, NY, USA) equipped with KBr windows and mounted on a Vertex 70 FTIR spectrometer (Bruker, Billerica, MA, USA) equipped with a liquid N<sub>2</sub>-cooled MCT detector. The monolithic aged catalysts were crushed and sieved to select particles between 40 and 80 μm. The fresh catalyst powder was degreened in the reactor set-up according to the procedure for the degreening pretreatment applied to each monolithic sample. Before the adsorption of probe molecules, the samples were dehydrated for 30 min in 8% O<sub>2</sub>/Ar at 500 °C followed with cooling to the adsorption temperature in Ar. The total flow was 50 mL/min. A background spectrum (48 scans) was recorded at each adsorption temperature under Ar flow. NH<sub>3</sub> adsorption was carried out at 150, 250, and 350 °C. The catalyst was exposed to 1000 ppm NH<sub>3</sub> for 30 min followed by 60 min flushing with argon (50 mL/min). Absorbance spectra (24 scans) were collected every 5 min to monitor the evolution of adsorbed species during the NH<sub>3</sub> step and subsequent Ar flushing. NO adsorption was carried out only at room temperature. To saturate the catalyst, 1000 ppm NO/Ar was fed for 20 min with a total flow of 50 mL/min.

## 4. Conclusions

In this study, we examined the deterioration of NH<sub>3</sub> SCR activity via rich aging of a Cu/SSZ-13 catalyst. The deactivation power of various realistic rich feeds and the effect of aging temperature were assessed. It was clear that aging is much worse in rich conditions than in lean ones. CO and H<sub>2</sub> showed a unique ability to modify the Cu species. In addition, a clear reduction of the number of acid sites was found after the aging and higher aging temperature led to greater drop of acid sites. Aging at 800 °C led to more severe deactivation for SCR and NH<sub>3</sub> oxidation than aging at 700 °C. Aging at 800 °C with 2000 ppm CO (and 10% H<sub>2</sub>O, 10% CO<sub>2</sub>, 500 ppm NO) led to SCR deactivation at low and, to a lesser extent, high temperatures. Aging in the presence of 2000 ppm H<sub>2</sub>, alone or in combination with CO, significantly lowered SCR activity in the whole temperature range (125–500 °C). After aging at 700 °C, the deactivation was limited to low temperatures (<250 °C) and was comparable for all rich conditions tested, including 222 ppm propene. Signs of SCR deactivation were observed after treatment at 600 °C in the presence of CO, which highlights the aging power of CO. NH<sub>3</sub> oxidation was also lowered, in general, by aging in rich conditions. Aging at 800 °C with CO was, however, an exception since it led to greater high-temperature NH<sub>3</sub> oxidation. The nature of Cu sites was investigated with DRIFT spectroscopy. NH<sub>3</sub> adsorption confirmed the important loss of Brønsted acid sites and isolated Cu<sup>2+</sup>. This indicates the enhanced dealumination and Cu cations mobility under rich conditions. Regarding the nature of Cu, DRIFT analyses showed an unusual increase in the ZCuOH/Z<sub>2</sub>Cu ratio brought about by aging in rich conditions. Studies of hydrothermal aging in lean conditions have all shown the conversion of ZCuOH to the more stable Z<sub>2</sub>Cu species. Aging in rich conditions was therefore more favorable to ZCuOH than lean conditions. This, possibly in combination

with the formation of Cu clusters, can be the cause of the more severe SCR deactivation under rich conditions than under lean conditions.

**Supplementary Materials:** The following is available online at <http://www.mdpi.com/2073-4344/9/11/929/s1>: Figure S1: SCR activity of all samples after degreening, i.e., before respective aging. Figure S2: SCR deactivation after 8 h lean aging at 700 °C.

**Author Contributions:** Conceptualization and methodology, X.A., O.M., B.L., and L.O.; investigation, formal analysis, writing and original draft preparation X.A.; writing, review, and editing, O.M., B.L., and L.O.

**Funding:** The authors gratefully acknowledge the funding from the Swedish Energy Agency, FFI, 44009-41, and the Swedish Research Council (642-2014-5733).

**Conflicts of Interest:** The authors declare no conflict of interest.

## References

1. Fickel, D.W.; D'Addio, E.; Lauterbach, J.A.; Lobo, R.F. The ammonia selective catalytic reduction activity of copper-exchanged small-pore zeolites. *Appl. Catal. B* **2011**, *102*, 441–448. [[CrossRef](#)]
2. Kwak, J.H.; Tonkyn, R.G.; Kim, D.H.; Szanyi, J.; Peden, C.H.F. Excellent activity and selectivity of Cu-SSZ-13 in the selective catalytic reduction of NO<sub>x</sub> with NH<sub>3</sub>. *J. Catal.* **2010**, *275*, 187–190. [[CrossRef](#)]
3. Xu, L.; McCabe, R.W. LNT in situ SCR catalyst system for diesel emissions control. *Catal. Today* **2012**, *184*, 83–94. [[CrossRef](#)]
4. Liu, Y.; Harold, M.P.; Luss, D. Coupled NO<sub>x</sub> storage and reduction and selective catalytic reduction using dual-layer monolithic catalysts. *Appl. Catal. B* **2012**, *121–122*, 239–251. [[CrossRef](#)]
5. Chatterjee, D.; Kočí, P.; Schmeißer, V.; Marek, M.; Weibel, M.; Krutzsch, B. Modelling of a combined NO<sub>x</sub> storage and NH<sub>3</sub>-SCR catalytic system for Diesel exhaust gas aftertreatment. *Catal. Today* **2010**, *151*, 395–409. [[CrossRef](#)]
6. Auvray, X.; Grant, A.; Lundberg, B.; Olsson, L. Lean and rich aging of a Cu/SSZ-13 catalyst for combined lean NO<sub>x</sub> trap (LNT) and selective catalytic reduction (SCR) concept. *Catal. Sci. Technol.* **2019**, *9*, 2152–2162. [[CrossRef](#)]
7. Huang, Y.; Cheng, Y.; Lambert, C. Deactivation of Cu/Zeolite SCR Catalyst Due To Reductive Hydrothermal Aging. *SAE Int. J. Fuels Lubr.* **2008**, *1*, 466–470. [[CrossRef](#)]
8. Kim, Y.J.; Kim, P.S.; Kim, C.H. Deactivation mechanism of Cu/Zeolite SCR catalyst under high-temperature rich operation condition. *Appl. Catal. A* **2019**, *569*, 175–180. [[CrossRef](#)]
9. Partridge, W.P.; Joshi, S.Y.; Pihl, J.A.; Currier, N.W. New operando method for quantifying the relative half-cycle rates of the NO SCR redox cycle over Cu-exchanged zeolites. *Appl. Catal. B* **2018**, *236*, 195–204. [[CrossRef](#)]
10. Paolucci, C.; Khurana, I.; Parekh, A.A.; Li, S.; Shih, A.J.; Li, H.; Di Iorio, J.R.; Albarracin-Caballero, J.D.; Yezerets, A.; Miller, J.T.; et al. Dynamic multinuclear sites formed by mobilized copper ions in NO<sub>x</sub> selective catalytic reduction. *Science* **2017**, *357*, 898–903. [[CrossRef](#)]
11. Luo, J.; Gao, F.; Kamasamudram, K.; Currier, N.; Peden, C.H.F.; Yezerets, A. New insights into Cu/SSZ-13 SCR catalyst acidity. Part I: Nature of acidic sites probed by NH<sub>3</sub> titration. *J. Catal.* **2017**, *348*, 291–299. [[CrossRef](#)]
12. Paolucci, C.; Parekh, A.A.; Khurana, I.; Di Iorio, J.R.; Li, H.; Albarracin Caballero, J.D.; Shih, A.J.; Anggara, T.; Delgass, W.N.; Miller, J.T.; et al. Catalysis in a Cage: Condition-Dependent Speciation and Dynamics of Exchanged Cu Cations in SSZ-13 Zeolites. *J. Am. Chem. Soc.* **2016**, *138*, 6028–6048. [[CrossRef](#)] [[PubMed](#)]
13. Kwak, J.H.; Zhu, H.; Lee, J.H.; Peden, C.H.F.; Szanyi, J. Two different cationic positions in Cu-SSZ-13? *Chem. Commun.* **2012**, *48*, 4758–4760. [[CrossRef](#)] [[PubMed](#)]
14. Borfecchia, E.; Lomachenko, K.A.; Giordanino, F.; Falsig, H.; Beato, P.; Soldatov, A.V.; Bordiga, S.; Lamberti, C. Revisiting the nature of Cu sites in the activated Cu-SSZ-13 catalyst for SCR reaction. *Chem. Sci.* **2015**, *6*, 548–563. [[CrossRef](#)]
15. Vallyon, J.; Hall, K. Studies of the surface species formed from NO on copper zeolites. *J. Phys. Chem.* **1993**, *97*, 1204–1212. [[CrossRef](#)]
16. Giordanino, F.; Vennestrøm, P.N.R.; Lundegaard, L.F.; Stappen, F.N.; Mossin, S.; Beato, P.; Bordiga, S.; Lamberti, C. Characterization of Cu-exchanged SSZ-13: A comparative FTIR, UV-Vis, and EPR study with Cu-ZSM-5 and Cu-β with similar Si/Al and Cu/Al ratios. *Dalton. Trans.* **2013**, *42*, 12741–12761. [[CrossRef](#)]

17. Concepción, P.; Boronat, M.; Millán, R.; Moliner, M.; Corma, A. Identification of Distinct Copper Species in Cu-CHA Samples Using NO as Probe Molecule. A Combined IR Spectroscopic and DFT Study. *Top. Catal.* **2017**, *60*, 1–11. [[CrossRef](#)]
18. Lezcano-Gonzalez, I.; Deka, U.; Arstad, B.; Van Yperen-De Deyne, A.; Hemelsoet, K.; Waroquier, M.; Van Speybroeck, V.; Weckhuysen, B.M.; Beale, A.M. Determining the storage, availability and reactivity of NH<sub>3</sub> within Cu-Chabazite-based Ammonia Selective Catalytic Reduction systems. *Phys. Chem. Chem. Phys.* **2014**, *16*, 1639–1650. [[CrossRef](#)]
19. Chen, L.; Falsig, H.; Janssens, T.V.W.; Jansson, J.; Skoglundh, M.; Grönbeck, H. Effect of Al-distribution on oxygen activation over Cu-CHA. *Catal. Sci. Technol.* **2018**, *8*, 2131–2136. [[CrossRef](#)]
20. Han, S.; Cheng, J.; Zheng, C.; Ye, Q.; Cheng, S.; Kang, T.; Dai, H. Effect of Si/Al ratio on catalytic performance of hydrothermally aged Cu-SSZ-13 for the NH<sub>3</sub>-SCR of NO in simulated diesel exhaust. *Appl. Surf. Sci.* **2017**, *419*, 382–392. [[CrossRef](#)]
21. Kim, Y.J.; Lee, J.K.; Min, K.M.; Hong, S.B.; Nam, I.S.; Cho, B.K. Hydrothermal stability of Cu/SSZ-13 for reducing NO<sub>x</sub> by NH<sub>3</sub>. *J. Catal.* **2014**, *311*, 447–457. [[CrossRef](#)]
22. Kwak, J.H.; Tran, D.; Burton, S.D.; Szanyi, J.; Lee, J.H.; Peden, C.H.F. Effects of hydrothermal aging on NH<sub>3</sub>-SCR reaction over Cu/zeolites. *J. Catal.* **2012**, *287*, 203–209. [[CrossRef](#)]
23. Leistner, K.; Kumar, A.; Kamasamudram, K.; Olsson, L. Mechanistic study of hydrothermally aged Cu/SSZ-13 catalysts for ammonia-SCR. *Catal. Today* **2018**, *307*, 55–64. [[CrossRef](#)]
24. Luo, J.; Wang, D.; Kumar, A.; Li, J.; Kamasamudram, K.; Currier, N.; Yezerets, A. Identification of two types of Cu sites in Cu/SSZ-13 and their unique responses to hydrothermal aging and sulfur poisoning. *Catal. Today* **2016**, *267*, 3–9. [[CrossRef](#)]
25. Schmieg, S.J.; Oh, S.H.; Kim, C.H.; Brown, D.B.; Lee, J.H.; Peden, C.H.F.; Kim, D.H. Thermal durability of Cu-CHA NH<sub>3</sub>-SCR catalysts for diesel NO<sub>x</sub> reduction. *Catal. Today* **2012**, *184*, 252–261. [[CrossRef](#)]
26. Wang, J.; Peng, Z.; Qiao, H.; Han, L.; Bao, W.; Chang, L.; Feng, G.; Liu, W. Influence of aging on in situ hydrothermally synthesized Cu-SSZ-13 catalyst for NH<sub>3</sub>-SCR reaction. *RSC Adv.* **2014**, *4*, 42403–42411. [[CrossRef](#)]
27. Rizzotto, V.; Chen, P.; Simon, U. Mobility of NH<sub>3</sub>-Solvated CuII Ions in Cu-SSZ-13 and Cu-ZSM-5 NH<sub>3</sub>-SCR Catalysts: A Comparative Impedance Spectroscopy Study. *Catalysts* **2018**, *8*, 162. [[CrossRef](#)]
28. De-La-Torre, U.; Pereda-Ayo, B.; Moliner, M.; González-Velasco, J.R.; Corma, A. Cu-zeolite catalysts for NO<sub>x</sub> removal by selective catalytic reduction with NH<sub>3</sub> and coupled to NO storage/reduction monolith in diesel engine exhaust aftertreatment systems. *Appl. Catal. B* **2016**, *187*, 419–427. [[CrossRef](#)]
29. Leistner, K.; Xie, K.; Kumar, A.; Kamasamudram, K.; Olsson, L. Ammonia Desorption Peaks Can Be Assigned to Different Copper Sites in Cu/SSZ-13. *Catal. Lett.* **2017**, *147*, 1882–1890. [[CrossRef](#)]
30. Song, J.; Wang, Y.; Walter, E.D.; Washton, N.M.; Mei, D.; Kovarik, L.; Engelhard, M.H.; Proding, S.; Wang, Y.; Peden, C.H.F.; et al. Toward Rational Design of Cu/SSZ-13 Selective Catalytic Reduction Catalysts: Implications from Atomic-Level Understanding of Hydrothermal Stability. *ACS Catal.* **2017**, *7*, 8214–8227. [[CrossRef](#)]
31. Shan, Y.; Shi, X.; Yan, Z.; Liu, J.; Yu, Y.; He, H. Deactivation of Cu-SSZ-13 in the presence of SO<sub>2</sub> during hydrothermal aging. *Catal. Today* **2019**, *320*, 84–90. [[CrossRef](#)]
32. Niwa, M.; Nishikawa, S.; Katada, N. IRMS-TPD of ammonia for characterization of acid site in  $\beta$ -zeolite. *Microporous Mesoporous Mater.* **2005**, *82*, 105–112. [[CrossRef](#)]
33. Ma, L.; Cheng, Y.; Cavataio, G.; McCabe, R.W.; Fu, L.; Li, J. In situ DRIFTS and temperature-programmed technology study on NH<sub>3</sub>-SCR of NO<sub>x</sub> over Cu-SSZ-13 and Cu-SAPO-34 catalysts. *Appl. Catal. B* **2014**, *156–157*, 428–437. [[CrossRef](#)]
34. Brookshear, D.W.; Nam, J.G.; Nguyen, K.; Toops, T.J.; Binder, A. Impact of sulfation and desulfation on NO<sub>x</sub> reduction using Cu-chabazite SCR catalysts. *Catal. Today* **2015**, *258*, 359–366. [[CrossRef](#)]
35. Ruggeri, M.P.; Nova, I.; Tronconi, E.; Pihl, J.A.; Toops, T.J.; Partridge, W.P. In-situ DRIFTS measurements for the mechanistic study of NO oxidation over a commercial Cu-CHA catalyst. *Appl. Catal. B* **2015**, *166*, 181–192. [[CrossRef](#)]
36. Szanyi, J.; Kwak, J.H.; Zhu, H.; Peden, C.H.F. Characterization of Cu-SSZ-13 NH<sub>3</sub> SCR catalysts: An in situ FTIR study. *Phys. Chem. Chem. Phys.* **2013**, *15*, 2368–2380. [[CrossRef](#)]

37. Zhang, R.; McEwen, J.-S.; Kollár, M.; Gao, F.; Wang, Y.; Szanyi, J.; Peden, C.H.F. NO Chemisorption on Cu/SSZ-13: A Comparative Study from Infrared Spectroscopy and DFT Calculations. *ACS Catal.* **2014**, *4*, 4093–4105. [[CrossRef](#)]
38. Cheung, T.; Bhargava, S.K.; Hobday, M.; Fogger, K. Adsorption of NO on Cu exchanged zeolites, an FTIR study: Effects of Cu levels, NO pressure, and catalyst pretreatment. *J. Catal.* **1996**, *158*, 301–310. [[CrossRef](#)]
39. Zones, S.I. Conversion of faujasites to high-silica chabazite SSZ-13 in the presence of N,N,N-trimethyl-1-adamantammonium iodide. *J. Chem. Soc. Faraday Trans.* **1991**, *87*, 3709–3716. [[CrossRef](#)]



© 2019 by the authors. Licensee MDPI, Basel, Switzerland. This article is an open access article distributed under the terms and conditions of the Creative Commons Attribution (CC BY) license (<http://creativecommons.org/licenses/by/4.0/>).